Bioflavonoids have also been reported to be involved in cell cycle regulation. For example, Quercetin was found to downregulate the expression of mutant p53 protein in human breast cancer cell lines, leading to an arrest of the cells in the G2–M phase of the cell cycle [21]. In the case of human leukemic T-cells, Quercetin was found to arrest the cells in late G1 phase. In addition, Luteolin has been reported to arrest the cell cycle in the G1 phase of human melanoma cells [22], and Genistein induces cell cycle arrest at the G2–M stage and the inhibition of cdc2 kinase activity [23]. The arrest of the cell cycle in turn reduces cell growth and results in apoptosis induction.

Another explanation for the anti-cancer activity of bioflavonoids is suggested by their ability to interact with hormone receptors [21]. Certain bioflavonoids have been reported to bind to estrogen binding sites in estrogen receptors, there by interrupting estrogen binding. Indeed, flavonoids, such as Daidzein, Genistein, Quercetin, and Luteolin, were found to suppress the induction of the proliferation-stimulating activity of environmental estrogens in human breast cancer cell lines [24]. However, whether estrogen binding induces the proliferation of leukemic cells has not been reported. Alternatively, flavonoids may interact with the binding sites of growth factors other than estrogen, thereby inhibiting the growth of leukemia cells.

In conclusion, dietary bioflavonoids exhibited an apoptosis-inducing effect in various human leukemia cells. Although further studies must be performed to elucidate the mechanism by which bioflavonoids induce apoptosis in leukemia cells, the present data indicates that dietary bioflavonoids might be useful chemotherapeutic reagents for leukemia patients.

Acknowledgements

We thank S. Yamauchi for her excellent secretarial work. We also thank Dr. Y. Matsuo (Hayashibara Biochemical Laboratories Inc.) for gifting the cell lines. This work was supported in part by Health and Labour Sciences Research Grants from the Ministry of Health, Labour and Welfare of Japan, MEXT. KAKENHI 15019129, JSPS. KAKENHI 15390133 and 15590361, grant from the Japan Health Sciences Foundation for Research on Health Sciences Focusing on Drug Innovation, a grant from Sankyo Foundation of Life Science.

Contributions: J. Matsui contributed to the concept and design, interpreted and analyzed the data, provided drafting of the article, and gave final approval. N. Kiyokawa contributed to the concept and design, interpreted and analyzed the data, provided drafting of the article, and gave final approval, and obtained a funding source. H. Takenouchi interpreted and analyzed the data, provided critical revisions and important intellectual content. T. Taguchi and K. Suzuki interpreted and analyzed the data. Y. Shiozawa provided administrative support, provided critical revisions and important intellectual content. M. Saito and W.-R. Tang provided administrative support. H. Okita provided critical revisions and important intellectual content. J. Fujimoto provided critical revisions and important intellectual content, and obtained a funding source.

References

[1] Havsteen B. Flavonoids, a class of natural products of high pharmacological potency. Biochem Pharmacol 1983;32:1141–8.
[2] Wollenweber E. Occurrence of flavonoid aglycones in medicinal plants. Prog Clin Biol Res 1988;280:45–55.
[3] Cody V. Crystal and molecular structures of flavonoids. Prog Clin Biol Res 1988;280:29–44.
[4] Vrijsen R, Everaert L, Boeye A. Antiviral activity of flavones and potentiation by ascorbate. J Gen Virol 1988;69:1749–51.
[5] Mittra B, Saha A, Chowdhury AR, Pal C, Mandal S, Mukhopadhyay S, et al. Luteolin, an abundant dietary component is a potent anti-leishmanial agent that acts by inducing topoisomerase II-mediated kinetoplast DNA cleavage leading to apoptosis. Mol Med 2000;6:527–41.
[6] Yoshida M, Sakai T, Hosokawa N, Marui N, Matsumoto K, Fujioka A, et al. The effect of Quercetin on cell cycle progression and growth of human gastric cancer cells. FEBS Lett 1990;260:10–3.
[7] Record IR, Broadbent JL, King RA, Dreosti IE, Head RJ, Tonkin AL. Genistein inhibits growth of B16 melanoma cells in vivo and in vitro and promotes differentiation in vitro. Int J Cancer 1997;72:860–4.
[8] Huang YT, Hwang JJ, Lee PP, Ke FC, Huang JH, Huang CJ, et al. Effects of Luteolin and Quercetin, inhibitors of tyrosine kinase, on cell growth and metastasis-associated properties in A431 cells overexpressing epidermal growth factor receptor. Br J Pharmacol 1999;128:999–1010.
[9] Ferry DR, Smith A, Malkhandi J, Fyfe DW, deTakats PG, Anderson D, et al. Phase I clinical trial of the flavonoid quercetin: pharmacokinetics and evidence for in vivo tyrosine kinase inhibition. Clin Cancer Res 1996;2:659–68.
[10] Mohammad RM, Al-Katib A, Aboukameel A, Doerge DR, Sarkar F, Kucuk O. Genistein sensitizes diffuse large cell lymphoma to CHOP (cyclophosphamide, doxorubicin, vincristine, prednisone) chemotherapy. Mol Cancer Ther 2003;2:1361–8.
[11] Pegoraro L, Matera L, Ritz J, Levis A, Palumbo A, Biagini G. Establishment of a Ph1-positive human cell line (BV-173). J Natl Cancer Inst 1983;70:447–53.
[12] Tsuganezawa K, Kiyokawa N, Matsuo Y, Kitamura F, Toyama-Sorimachi N, Kuida K, et al. Flow cytometric diagnosis of the cell lineage and developmental stage of acute lymphoblastic leukemia by novel monoclonal antibodies specific to human pre B cell receptor. Blood 1998;92:4317–24.
[13] Kiyokawa N, Kokai Y, Ishimoto K, Fujita H, Fujimoto J, Hata J. Characterization of the common acute lymphoblastic leukemia antigen (CD10) as an activation molecule on mature human B cells. Clin Exp Immunol 1990;79:322–7.
[14] Chowdhury AR, Sharma S, Mandal S, Goswami A, Mukhopadhyay S, Majumder HK. Luteolin, an emerging anti-cancer flavonoid, poisons eukaryotic DNA topoisomerase I. Biochem J 2002;366:653–61.
[15] Strick R, Strissel PL, Borgers S, Smith SL, Rowley JD. Dietary bioflavonoids induce cleavage in the MLL gene and may contribute to infant leukaemia. Proc Natl Acad Sci USA 2000;97:4790–5.
[16] Liu LF. DNA topoisomerase poisons as antitumor drugs. Annu Rev Biochem 1989;58:351–75.
[17] Beere HM, Chresta CM, Alejo-Herberg A, Skladanowski A, Dive C, Larsen AK, et al. Investigation of the mechanism of higher order chromatin fragmentation observed in drug-induced apoptosis. Mol Pharmacol 1995;47:986–96.

[18] Chandra D, Choy G, Deng X, Bhatia B, Daniel P, Tang DG. Association of active caspase 8 with the mitochondrial membrane during apoptosis: potential roles in cleaving BAP31 and caspase 3 and mediating mitochondrion-endoplasmic reticulum cross talk in etoposide-induced cell death. Mol Cell Biol 2004;24:6592–607.

[19] Strissel PL, Strick R, Rowley JD, Zeleznik-Le NJ. An in vivo topoisomerase II cleavage site and a DNase I hypersensitive site colocalize near exon 9 in the MLL breakpoint cluster region. Blood 1998;92:3793–803.

[20] Martins LM, Mesner PW, Kottke TJ, Basi GS, Sinha S, Tung JS, et al. Comparison of caspase activation and subcellular localization in HL-60 and K562 cells undergoing etoposide-induced apoptosis. Blood 1997;90:4283–96.

[21] Lamson DW, Brignall MS. Antioxidants and cancer, part 3: quercetin. Altern Med Rev 2000;5:196–208.

[22] Casagrande F, Darbon JM. Effects of structurally related flavonoids on cell cycle progression of human melanoma cells: regulation of cyclin-dependent kinases CDK2 and CDK1. Biochem Pharmacol 2001;61:1205–15.

[23] Su SJ, Yeh TM, Lei HY, Chow NH. The potential of soybean foods as a chemoprevention approach for human urinary tract cancer. Clin Cancer Res 2000;6:230–6.

[24] Han DH, Denison MS, Tachibana H, Yamada K. Relationship between estrogen receptor-binding and estrogenic activities of environmental estrogens and suppression by flavonoids. Biosci Biotechnol Biochem 2002;66:1479–87.

Primary Malignant Lymphoma of the Central Nervous System in an Immunocompetent Child

A Case Report

Yusuke Shiozawa, MD,† Nobutaka Kiyokawa, MD,† Junya Fujimura, MD,* Kyoko Suzuki, MD,* Yukiko Yarita, MD,* Junichiro Fujimoto, MD,† Masahiro Saito, MD,* and Yuichiro Yamashiro, MD**

Summary: Primary lymphoma of the central nervous system (PCNSL) is extremely rare, especially in childhood. A 9-year-old Japanese boy was diagnosed as having precursor-B cell-type lymphoblastic lymphoma, based on morphologic and immunocytochemical analysis of mononuclear cells in the cerebrospinal fluid and a positive reaction for terminal deoxynucleotidyl transferase (TdT), CD19, CD79a, and CD179b. After seven courses of chemotherapy and craniospinal radiotherapy, the patient is alive, well, and in continuous complete remission. Despite its rarity, PCNSL should be included in the differential diagnosis in the presence of symptoms of increased intracranial pressure and/or unusual imaging findings of the brain.

Key Words: central nervous system, lymphoma, childhood, immunohistochemical examination, cerebrospinal fluid

(*J Pediatr Hematol Oncol* 2005;27:561–564)

Although malignant lymphomas may extend to the central nervous system (CNS) in cases of advanced disease, primary CNS lymphoma (PCNSL) is extremely rare, especially in childhood. It represents less than 2% of all primary brain tumors and approximately 1% to 2% of all cases of malignant lymphoma.[1] Schulman et al reported that PCNSL is a disease of the fourth to sixth decade of life and is rare during the first decade of life.[2]

In recent reports, the incidence of PCNSL among not only immunocompetent but also immunocompromised patients has increased because of the increased prevalence of AIDS and the growing number of organ transplantations.[1,3,4]

The prognosis of PCNSL is poor, despite the combination of aggressive radiotherapy and chemotherapy.[1,3,4] Because of its rarity, the incidence and prognosis of PCNSL in childhood are not recognized. We report a case of PCNSL in an immunocompetent child, in which immunohistochemical examination of the cerebrospinal fluid (CSF) was helpful for the diagnosis.

CASE REPORT

A 9-year-old Japanese boy had complained of headache followed by nausea and vomiting for 1 month. CT of the brain was performed at a local hospital and a high-density lesion on the left occipital lobe was noted. He was then referred to our hospital for further evaluation and treatment with the suspected diagnosis of a brain tumor. He had been in good health and had no history of congenital immunodeficiency disease, previous organ transplantation, immunosuppressive therapy, or AIDS. The family history was unremarkable for cancer or any immunodeficiency disease.

On physical examination on admission, the patient was alert and had no fever, lymphadenopathy, hepatosplenomegaly, or any other abnormal findings, including the CNS. Complete blood count showed a white blood cell count of 8,100/μL with normal differential, hemoglobin 13.9 g/dL, and platelets 273,000/μL. Bone marrow aspiration was normal. Lumber puncture showed leukocytes 184/μL with atypical cells, protein 18 mg/dL, and glucose 49 mg/dL. In the immunocytochemistry studies, atypical CSF cells showed a positive reaction for terminal deoxynucleotidyl transferase (TdT), CD19, CD79a, and CD179b but a negative reaction for CD45 (Fig. 1), a typical immunophenotype for precursor-B lymphoblastic lymphoma.[5] MRI showed a high-density lesion on the left occipital lobe (Fig. 2). Chest and abdominal CT scans were normal.

A diagnosis of precursor-B cell-type lymphoblastic lymphoma was made based on the morphologic and immunocytochemical analyses of mononuclear cells in the CSF. Treatment was started, including systemic high-dose intravenous methotrexate and high-dose cytarabine (Ara-C), combined with triple intrathecal chemotherapy (methotrexate, hydrocortisone, and Ara-C) and craniospinal radiotherapy (Table 1). After two courses of chemotherapy, the patient was in complete remission as assessed by MRI (see Fig. 2) and CSF cytology. Twenty-two months after treatment was started, a total of seven courses of chemotherapy and craniospinal radiotherapy (total 24 Gy) had been given, and the patient is alive, well, and in continuous complete remission.

DISCUSSION

Although the incidence of PCNLS has increased over the past two or three decades, PCNLS in immunocompetent patients is still rare. In fact, only a few series of PCNLS in immunocompetent patients have been reported. The incidence of PCNLS in childhood is in particular extremely low: only 3 cases in patients younger than 10 years old were listed out of a total of 76 immunocompetent cases reported from

Received for publication February 29, 2004; accepted August 23, 2005.

From the *Department of Pediatrics, Juntendo University, School of Medicine, Tokyo, Japan; and †Department of Developmental Biology, National Research Institute for Child Health and Development, Tokyo, Japan.

Reprints: Yusuke Shiozawa, Department of Pediatrics, Juntendo University, School of Medicine, 2-1-1 Hongo, Bunkyou-ku, Tokyo #113-8421, Japan (e-mail: y-shio@mte.biglobe.ne.jp).

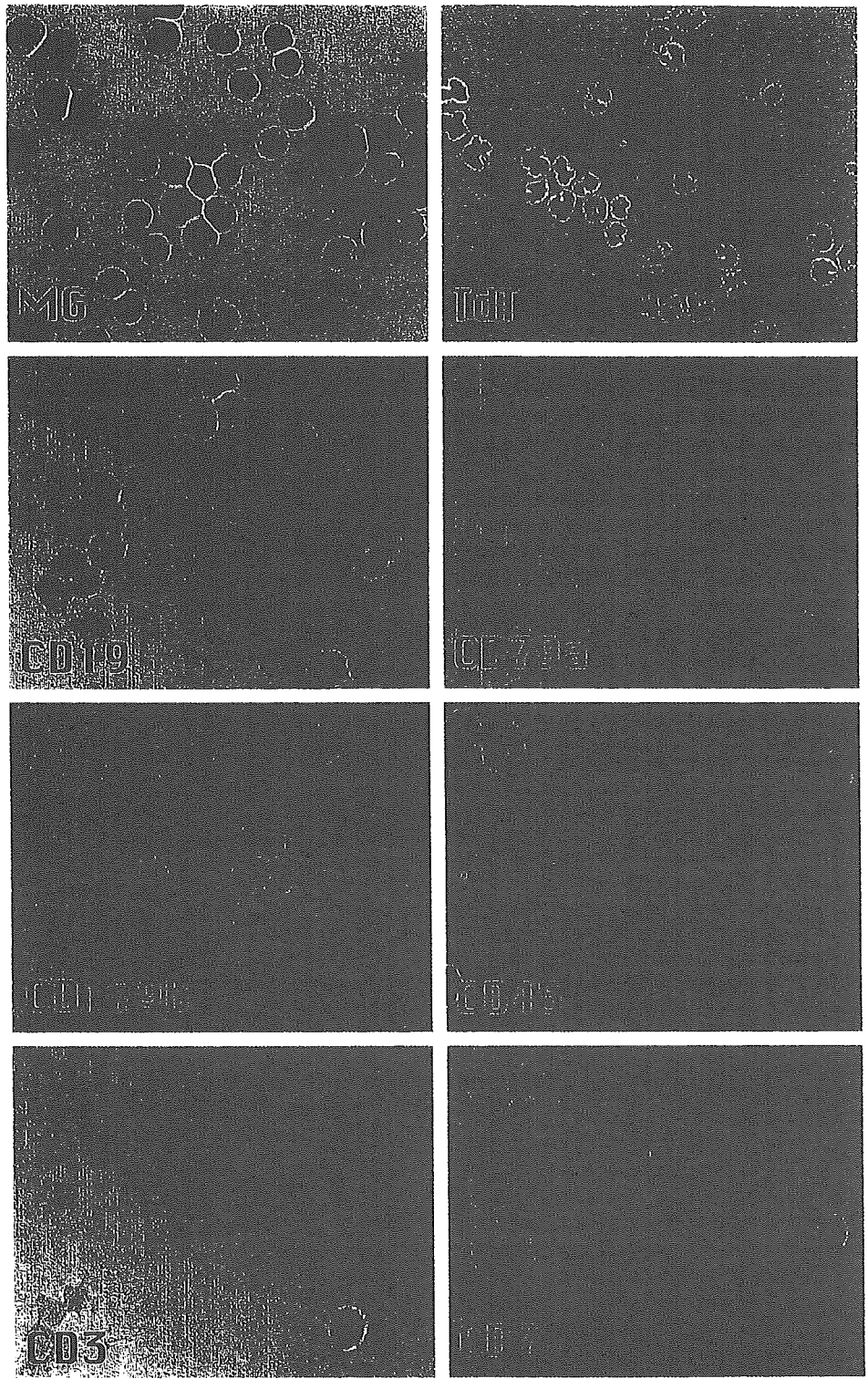

FIGURE 1. Immunohistochemical analysis of the CSF cells. The CSF cells obtained from the patient by lumber puncture were cytocentrifuged on slide glasses using Cytospin III (Shandon Scientific Ltd, Pittsburgh, PA). After fixation with acetone, immunohistochemical staining was performed according to the standard procedure using antibodies indicated in the figure. TdT, CD19, CD79a, and CD179b were mostly positive, whereas weak staining with CD79a was seen. CD45, CD3, and CD7 were mostly negative.

a combination of the data from four series.[6–9] Despite its rarity, however, PCNSL should be included in the differential diagnosis in the presence of seizures and symptoms of increased intracranial pressure such as headache, nausea, and vomiting and/or unusual imaging findings of the brain.

In making a correct diagnosis of PCNSL, leptomeningeal biopsy is considered the most important diagnostic procedure, but it is not easily performed because of its invasive nature. On the other hand, when a tumor involves the leptomeninges or the ventricles, malignant cells are often

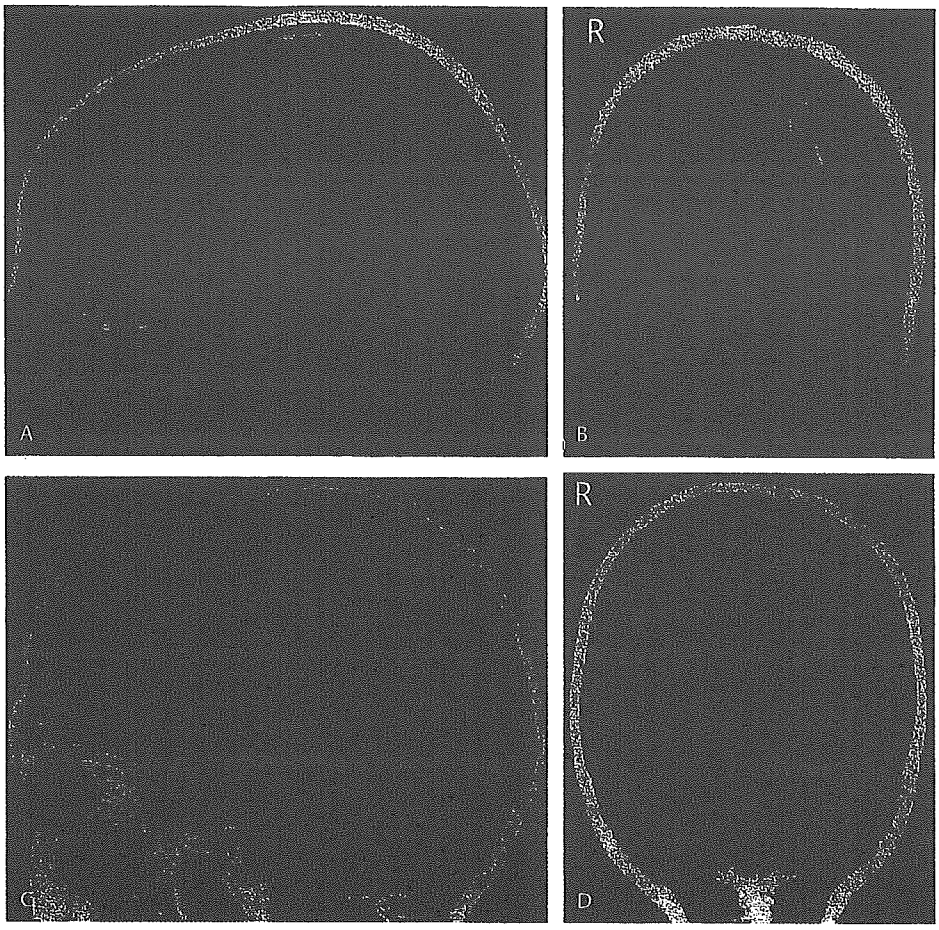

FIGURE 2. A, B, Sagittal and coronal T1-weighted MRI scan showed a high-density lesion on the left occipital lobe. C, D, Sagittal and coronal T1-weighted MRI scan became normal after chemotherapy.

readily identifiable in the CSF, and thus CSF involvement in lymphoma and leukemia is well recognized.[10,11] Although the frequency of CSF involvement in PCNSL at the time of diagnosis varies according to the literature, it is supposed to be approximately 40%.[4] Because lumbar puncture is safe in comparison with biopsy, cytologic examination of the CSF should be a useful diagnostic procedure in PCNSL patients. Typical CSF analysis in PCNSL patients reveals an increase in the white blood cells[11] and proteins,[4] although glucose is often normal;[4] however, these findings do not necessarily indicate a diagnosis of lymphoma.[11] Therefore, the detection of lymphoma cells is critical for the diagnosis. However, sometimes in case of lymphoma only a few abnormal cells are shed into the CSF. Therefore, the diagnosis of lymphoma from the CSF findings can be difficult because of the presence of normal or reactive lymphocytes, or a small number cells in the sample.[11] In addition, because normal cell counts do not necessarily exclude lymphoma,[11] biopsy should still be considered the standard diagnostic procedure for PCNSL. However, in such cases, the application of immunocytochemistry can strongly assist in detecting lymphoma cells.[10,12]

Although the specific markers for malignant cells are not present, the detection of unusual markers for CSF cells should provide strong evidence for the diagnosis of lymphoma. In our patient, the immunohistochemical examination of CSF revealed the presence of cells that expressed CD19, CD79a, CD179b, and TdT, but not CD45. TdT and CD179b are specific markers for lymphoid precursors and B-cell precursors, respectively.[5] Together with the expression of CD19 and CD79a, an increase in B-cell precursors in the CSF was suggested. Because B-cell precursors are never present in CSF in normal or reactive conditions, the above data strongly indicated a diagnosis of B-precursor lymphoblastic lymphoma. Although CD45 is known to be a leukocyte-common antigen, it is well established that B-precursor neoplasms exhibit an absence or a low-level expression of this marker. Therefore, the lack of CD45 further supported the diagnosis of B-precursor lymphoblastic lymphoma. Based on the above findings, a diagnosis of PCNSL could be made safely with the immunohistochemical examination of the CSF, and appropriate treatment could be started. Thus, we emphasize that when PCNSL is suspected from the clinical findings, imaging, and so on, cytologic examination of the CSF using immunocytochemical techniques should be performed first.

The prognosis of PCNSL is poor. Established lymphoma chemotherapy regimens for non-CNS disease are ineffective for the treatment of PCNSL, which requires a specialized approach that takes into consideration a disease protected by an intact blood–brain barrier.[3] Although there is no uniform approach to the treatment of PCNSL at this moment,

TABLE 1. Chemotherapy Regimen

Week 1	Week 2	Week 6	Week 10	Week 14	Week 18	Week 22	Week 26
Block 1	Block 2	Block 3	Block 3	Block 4	Block 2	Block 2	Block 4
▲ ▲	▲	▲ △	▲ △	▲ △	△	△	△
					⟷ Cranial irradiation (24 Gy)		

Block 1	Etoposide	100 mg/m^2	day 5–6
	Prednisolone (PO)	60 mg/m^2 (max: 80 mg)	day 1–7
Block 2	Vincristine	1.5 mg/m^2 (max: 2 mg)	day 1
	Cytarabine	150 mg/m^2 × 2/day	day 1–4
	Cyclophosphamide	1 g/m^2	day 2–4
	Epirubicin	80 mg/m^2	day 5
	Dexamethasone (PO)	10 mg/m^2 (max: 10 mg)	day 1–5
Block 3	Cyclophosphamide	300 mg/m^2 × 2/day	day 2–4
	Etoposide	100 mg/m^2	day 2–5
	Methotrexate	3 g/m^2 (24 h d.i.v.)	day 1
	Epirubicin	80 mg/m^2	day 5
	Dexamethasone (PO)	10 mg/m^2 (max: 10 mg)	day 1–5
Block 4	Vindesine	3 mg/m^2	day 1
	Etoposide	100 mg/m^2	day 2–5
	Cytarabine	2 mg/m^2 × 2/day	day 1–3
	Epirubicin	80 mg/m^2	day 5
	Dexamethasone (PO)	10 mg/m^2 (max: 10 mg)	day 1–5

Intrathecal Chemotherapy					
▲	Methotrexate	12.5 mg	△	Methotrexate	12.5 mg
	Cytarabine	25 mg		Hydrocortisone	25 mg
	Hydrocortisone	25 mg			

chemotherapy containing high-dose methotrexate and/or high-dose Ara-C with intrathecal methotrexate and Ara-C followed by craniospinal radiotherapy has been recommended.[3,4] However, although intravenous methotrexate, intrathecal methotrexate, and craniospinal radiotherapy each have the potential for producing leukoencephalopathy independently, when two or three of these treatment modalities are added together, the risk will increase.[3] Craniospinal radiotherapy doses greater than 50 Gy carry a high risk of postirradiation leukoencephalopathies in long-term survivors.[1] Thus, the role of craniospinal radiotherapy in the primary therapy for PCNSL has still not been clearly defined. In our patient, because intravenous methotrexate, intrathecal methotrexate, and craniospinal radiotherapy had already been used, follow-up over the long term while keeping a careful watch for leukoencephalopathy is required.

Because PCNSL is extremely rare in immunocompetent children, well-designed, prospective, randomized, and multicenter clinical trials are needed to improve the prognosis of PCNSL and to define successful treatment strategies.

REFERENCES

1. Bataille B, Delwail V, Menet E, et al. Primary intracerebral malignant lymphoma: report of 248 cases. *J Neurosurg.* 2000;92:261–266.
2. Schulman H, Hertzanu Y, Maor E, et al. Primary lymphoma of brain in childhood. *Pediatr Radiol.* 1991;21:434–435.
3. Plasswilm L, Herrlinger U, Korfel A, et al. Primary central nervous system (CNS) lymphoma in immunocompetent patients. *Ann Hematol.* 2002;81:415–423.
4. Basso U, Brandes AA. Diagnostic advances and new trends for the treatment of primary central nervous system lymphoma. *Eur J Cancer.* 2002;38:1298–1312.
5. Kiyokawa N, Sekino T, Matsui T, et al. Diagnostic importance of CD179a/b as markers of precursor B-cell lymphoblastic lymphoma. *Mod Pathol.* 2004;27:423–429.
6. Jiddane M, Nicoli F, Diaz P, et al. Intracranial malignant lymphoma. Report of 30 cases and review of literature. *J Neurosurg.* 1986;65:592–599.
7. Vakili ST, Muller J, Shidnia H, et al. Primary lymphoma of the central nervous system: A clinicopathologic analysis of 26 cases. *J Surg Oncol.* 1986;33:95–102.
8. Lachance DH, O'Neill BP, Macdonald DR, et al. Primary leptomeningeal lymphoma: report of 9 cases, diagnosis with immunocytochemical analysis, and review of the literature. *Neurology.* 1991;41:95–100.
9. Sheikh B, Siqueira E. Primary lymphoma of the central nervous system. *Br J Neurosurg.* 1994;8:427–432.
10. Tani E, Costa I, Svedmyr E, et al. Diagnosis of lymphoma, leukemia, and metastatic tumor involvement of the cerebrospinal fluid by cytology and immunocytochemistry. *Diagn Cytopathol.* 1995;12:14–22.
11. Roma AA, Garcia A, Avagnina A, et al. Lymphoid and myeloid neoplasms involving cerebrospinal fluid: comparison of morphologic examination and immunophenotyping by flow cytometry. *Diagn Cytopathol.* 2002;27:271–275.
12. Chhieng DC, Elgert P, Cohen J-M, et al. Cytology of primary central nervous system neoplasms in cerebrospinal fluid specimens. *Diagn Cytopathol.* 2002;26:209–212.

ELSEVIER

EXPERIMENTAL HEMATOLOGY

Experimental Hematology ■ (2006) ■

Involvement of insulin-like growth factor-I and insulin-like growth factor binding proteins in pro–B-cell development

Tomoko Taguchi[a,b], Hisami Takenouchi[a,b], Jun Matsui[a], Wei-Ran Tang[a], Mitsuko Itagaki[a], Yusuke Shiozawa[a], Kyoko Suzuki[a], Sachi Sakaguchi[a], Yohko U. Ktagiri[a], Takao Takahashi[b], Hajime Okita[a], Junichiro Fujimoto[a], and Nobutaka Kiyokawa[a]

[a]*Department of Developmental Biology, National Research Institute for Child Health and Development, Setagaya-ku, Tokyo;* [b]*Department of Pediatrics, Keio University, School of Medicine, Shinjuku-ku, Tokyo, Japan*

(Received 14 March 2005; revised 12 December 2005; accepted 12 January 2006)

Objective. **Insulin-like growth factor (IGF)-binding proteins (IGFBPs) are a family of proteins thought to modulate IGF function. By employing an in vitro culture system of human hematopoietic stem cells cocultured with murine bone marrow stromal cells, we examined the effects of IGF-I and IGFBPs on early B-cell development.**

Materials and Methods. **Human CD34$^+$ bone marrow cells were cocultured with murine stromal MS-5 cells for 4 weeks, and pro–B-cell number was analyzed by flow cytometry. After administration of reagents that are supposed to modulate IGF-I or IGFBP function to the culture, the effect on pro–B-cell development was examined.**

Results. **After cultivation for 4 weeks, effective induction of pro–B-cell proliferation was observed. Experiments using several distinct factors, all of which neutralize IGF-I function, revealed that impairment of IGF-I function results in a significant reduction in pro–B-cell development from CD34$^+$ cells. In addition, when the effect of recombinant proteins of IGFBPs and antibodies against IGFBPs were tested, IGFBP-3 was found to inhibit pro–B-cell development, while IGFBP-6 was required for pro–B-cell development.**

Conclusions. **IGF-I is essential for development of bone marrow CD34$^+$ cells into pro-B cells. Moreover, IGFBPs are likely involved in regulation of pro–B-cell development.** © **2006 International Society for Experimental Hematology. Published by Elsevier Inc.**

Insulin-like growth factor-I (IGF-I) is an anabolic hormone and, like growth hormone and insulin, regulates whole body growth, metabolism, tissue repair, and cell survival [1]. In addition to its main production by the liver, IGF-I is also produced by bone marrow (BM) stromal cells, myeloid cells, and peripheral lymphocytes. In plasma and most biological fluids, IGF-I binds to members of a family of six specific soluble proteins, known as IGF-binding proteins (IGFBPs) 1–6, all of which have structures that are unrelated to those of IGF receptors (IGFRs) [2]. Although IGFBPs were originally described as passive circulating transport proteins, they are now recognized as playing a variety of roles in circulation, the extracellular environment, and inside the cell [3,4].

Offprint requests to: Tomoko Taguchi, M.D., Ph.D., Department of Developmental Biology, National Research Institute for Child Health and Development, 2-10-1, Okura, Setagaya-ku, Tokyo 154-8535, Japan; E-mail: ttaguchi@nch.go.jp

Of the six IGFBPs, IGFBP-3 is the most abundant IGFBP in plasma. In vitro experiments examining the effects of IGFBP-3 on various cell cultures have provided conflicting data, with both enhancement and inhibition of IGF-I actions, depending upon the cell type and culture conditions used [3,4]. In contrast, IGFBP-6 was purified from human cerebrospinal fluid and from transformed human fibroblast cell culture [3]. IGFBP-6 has been shown to inhibit IGF actions, including proliferation, differentiation, cell adhesion, and colony formation of osteoblasts and myoblasts [4]. Although the IGFBPs differ in their structure and binding specificity, functional differences among the various IGFBPs are still not clear [4].

In view of its multiple effects, IGF-I is thought to play an integral role in hematopoiesis [1]. IGF-I stimulates growth of bones and seems to control the volume of BM, thereby regulating production of hematopoietic cells [5]. Moreover, IGF-I has been suggested to have direct effects on development of a variety of hematopoietic cells. In the case of

[Q1] 0301-472X/06 $–see front matter.
doi: 10.1016/j.exphem.2006.01.009

B-cell development in mice, for example, previous reports have indicated that IGF-I stimulates maturation of pro-B cells into pre-B cells [6] and acts as a B-cell proliferation cofactor to synergize with the activity of interleukin (IL)-7 [7]. Indeed, administration of IGF-I increased the number of pre-B cells in BM and splenic B cells in normal mice and after BM transplantation [8]. However, the effect of IGF-I on B-cell development, especially in humans, is still largely unknown. In addition, although murine BM stromal cells secrete IGFBPs, the functional role of them in hematopoiesis remains unclear.

In an attempt to clarify the effect of IGF-I and IGFBPs on early B-cell development, we employed an in vitro culture system of human hematopoietic stem cells (HPSCs) cocultured with murine BM stromal cells that induce pro-B cells. In this article, we expand upon results of previous reports by other authors and show that IGF-I is essential for pro–B-cell induction from HPSCs. In addition, we also report that IGFBP-3 inhibits pro–B-cell development, whereas IGFBP-6 is required for pro–B-cell development. The possible role of IGFBPs in early B-cell development is discussed.

Materials and methods

Reagents

Recombinant human and mouse IGF-I, IGFBPs, and the IGF-IR kinase inhibitor I-OMe-AG538 were obtained from PeproTech EC Ltd. (London, UK), G-T Research Products (Minneapolis, MN, USA), and Calbiochem-Novabiochem Co. (San Diego, CA, USA), respectively. All reagents are solved in phosphate-buffered saline, except I-Ome-AG538, which is solved in dimethyl sulfoxide, and diluted to the indicated concentration by culture medium.

The following mouse monoclonal antibodies (mAbs) against human antigens were used: anti-IGF-IR from G-T; purified anti-CD19, fluorescein isothiocyanate (FITC)-conjugated anti-μ heavy chain, and phycoerythrin (PE)-conjugated anti-κ and anti-λ light chains and anti-CD25 from Becton Dickinson Biosciences (San Diego, CA, USA); FITC-conjugated anti-CD24, CD43, and CD45, PE-conjugated anti-CD10, CD20, CD33, and CD179a, and PE-cyanine (PC)-5–conjugated anti-CD19 from Beckman/Coulter Inc. (Westbrook, MA, USA). The CD179a molecule, also known as VpreB, is a component of surrogate light chain and is specifically expressed in B-cell precursors, including pro-B and pre-B cells, but not in mature B cells [9]. Hamster mAb against mouse IGF-I and goat polyclonal anti-mouse IGF-I, and IGFBPs Abs were obtained from G-T. Rabbit polyclonal Abs against human IGF-IR and phosphospecific IGF-IR were purchased from Cell Signaling Technology (Beverly, MA, USA). Goat polyclonal anti–β-actin Ab was obtained from Santa Cruz Biotechnology, Inc. (Santa Cruz, CA, USA). Secondary Abs were obtained from Molecular Probes, Inc. (Eugene, OR, USA), and Dako Cytomation, Co. (Glostrup, Denmark), respectively. All other chemical reagents were obtained from Wako Pure Chemical Industries, Ltd. (Osaka, Japan), unless otherwise indicated.

Cells and cultures

Human BM $CD34^+$ cells purchased from Cambrex Bio Science Walkersville, Inc. (Walkersville, MD, USA) were used. These cells had been isolated from human tissue after obtaining informed consent. A cloned murine BM stromal cell line, MS-5, was kindly provided by Dr. A. Manabe (St. Luke's International Hospital, Tokyo, Japan) and Dr. K. J. Mori (Nigata University, Nigata, Japan). Human B-precursor acute lymphoblastic leukemia cell line NALM-16 was kindly provided by Dr. Y. Matsuo (Grand Saule Immuno research Laboratory, Nara, Japan) and was maintained in RPMI-1640 supplemented with 10% (v/v) fetal calf serum (FCS; Sigma-Aldrich Fine Chemical Co., St. Louis, MO, USA) at 37°C in a humidified 5% CO_2 atmosphere.

For induction of pro-B cells, MS-5 cells were plated at a concentration of 1×10^5 cells on a 12-well tissue plate (Asahi Techno Glass Co., Chiba, Japan). The next day, 4×10^4 cells/well/2 mL $CD34^+$ cells were plated onto the MS-5 cells in culture medium supplemented with 10% FCS and various combinations of reagents, as indicated in the figures. Because our preliminary experiments revealed that cultures in an RPMI-1640 medium produced a higher yield of B cells compared with cultures in α-minimum essential medium (data not shown), we used RPMI-1640 medium for the following experiments. After cultivation for the indicated periods, cells were harvested using 0.25% trypsin plus 0.02% ethylenediamine tetraacetic acid (IBL Co. Ltd., Gunma, Japan), and the number of cells per well was determined. All experiments were performed in triplicate, and means ± standard deviations (SD) of cell numbers are shown in the figures. For the histology studies, cells were cultured on type-I collagen-coated cover slips (Asahi Techno Glass) and were examined by May-Grünwald-Giemsa staining or immunohistochemical staining.

Immunofluorescence study

A multicolor immunofluorescence study was performed using a combination of FITC, PE, and PC-5. Cells were stained with fluorescence-labeled mAbs and analyzed by flow cytometry (EPICS-XL, Beckman/Coulter), as described previously [10]. Staining of the cytoplasmic antigens was performed using Cytofix/Cytoperm Kits (Becton Dickinson), according to manufacturer's protocol. To detect surface immunoglobulin $(Ig)^+$ mature B cells and cytoplasmic μ^+ pre-B cells simultaneously, cells were first stained with a mixture of PC-5-conjugated anti-CD19 Ab and PE-conjugated Abs against κ/λ light chains and then treated with cell permeabilization reagents followed by staining of cytoplasmic antigens. It was confirmed by preliminary experiments that permeabilization treatment does not affect the signals of surface antigens stained beforehand. For cell sorting, human BM $CD34^+$ cells cocultured with MS-5 for 4 weeks were harvested and stained with PC-5–conjugated anti-CD19 mAb. $CD19^+$ cells were sorted in an EPICS-ALTRA cell sorter (Beckman/Coulter). For CD19 immunostaining, cover slips were fixed with ice-cold acetone for 15 minutes and stained with anti-CD19 mAb and examined by confocal laser scanning microscope (FV500; Olympus, Tokyo, Japan) as described previously [11].

RT-PCR, immunoblotting, and detection of IGF-I

Total RNA was extracted from cultured cells, and reverse transcriptase polymerase chain reaction (RT-PCR) was performed as described previously [12]. The sets of primers used in this study are listed in Table 1. Cell lysates were prepared by solubilizing the cells in lysis buffer and immunoblotting was performed as described previously [13]. The concentration of mouse IGF-I in

Table 1. ■

Name of gene	Primer sequence forward reverse	Product size (bp)
human IGF-I	5′-ACAGGTATCGTGGATGAGTG-3′ 5′-GTAACTCGTGCAGAGCAAAG-3′	263
human IGF-IR	5′-ATGTGCTGGCAGTATAACCC-3′ 5′-ACAGCCTTGGATGAACGATG-3′	929
mouse IGF-I	5′-ATGCTCTTCAGTTCGTGTGT-3′ 5′-CTTCTCCTTTGCAGCTTCGT-3′	271
mouse IGFBP-1	5′-AGATTAGCTGCAGCCCAAC -3′ 5′-TGTTCTAGGCAGCATCACTCT-3′	535
mouse IGFBP-2	5′-ATCCCCAACTGTGACAAGCA-3′ 5′-CCTCTCTAACAGAAGCAAGGGA-3′	407
mouse IGFBP-3	5′-TCCAAGTTCCATCCACTCCA-3′ 5′-GAGGCAATGTACGTCGTCTT-3′	372
mouse IGFBP-4	5′-AATTAGAGATCGGAGCAAGA-3′ 5′-TGGGAATTCCTATTGCTACA-3′	598
mouse IGFBP-5	5′-ATGAGACAGGAATCCGAACA-3′ 5′-TCAACGTTACTGCTGTCGAA-3′	269
mouse IGFBP-6	5′-TGCTAATGCTGTTGTTCGCT-3′ 5′-TGAGTGCTTCCTTGACCATC-3′	652
human GAPDH	5′-CCACCCATGGCAAATTCCATGGCA-3′ 5′-TCTAGACGGCAGGTCAGGTCCACC-3′	598
mouse Actin	5′-TGACGGGGTCACCCACACTGTGCCCATCTA-3′ 5′-CTAGAAGCATTTGCGGTGGACGATGGAGGG-3′	661

culture supernatants of MS-5 cells was determined by sandwich enzyme-linked immunosorbent assay (ELISA), using Mouse IGF-I Quantikine ELISA Kit (R&D Systems, Wiesbaden, Germany), according to manufacturer's instruction. Experiments were performed in triplicate, and mean ± SDs of cell numbers are shown in the figures.

Results

Differentiation of pro-B cells from human BM CD34$^+$ cells by coculturing with murine stromal MS-5 cells

Murine stromal cell line MS-5 has been reported to possess the capability to support differentiation of B-lineage cells from human cord blood (CB) CD34$^+$ cells [14–17]. Coincident with these previous reports, we observed that human BM CD34$^+$ cells generated a high number of CD19$^+$ B cells after cocultivation with MS-5 cells (Fig. 1A and B). Starting with 4×10^4 CD34$^+$ cells, approximately 0.4 to 1.3×10^6 mononuclear cells, 30.1% to 68.2% of which were CD19$^+$ cells, were obtained after 4 weeks of cultivation. As shown in Figure 1C, approximately half of the hematopoietic cells were floating, while the remainder were adhered to the MS-5 cells and the CD19$^+$ cells were more abundant in adherent cell fraction.

As shown in Figure 1B, most of the CD19$^+$ B cells obtained after 9 weeks of cultivation expressed cytoplasmic CD179a. The CD179a is reported to be already expressed in pro-B cells, remains expressed on B-cell precursors, and disappears upon differentiation from pre-B cells to mature B cells [9]. In contrast, a few percent of CD19$^+$ cells were positive for surface and/or cytoplasmic μ heavy chain and a portion of them expressed either the κ or λ light chains (Fig. 1B). We also observed that CD10, CD24, CD43, and CD45 were expressed but CD20 and CD25 were not in the CD19$^+$ cells (Fig. 1D). No difference in immunophenotypic characteristics was observed between the CD19$^+$ cells in adherent cell fraction and that in floating cell fraction (data not shown). Based on the above data, we concluded that human BM CD34$^+$ cells can differentiate into pro-B cells, but not into pre-B cells, after coculturing with the murine stromal cell line MS-5 in the present culture system. CD19$^+$ cells cultured for 4 weeks were also examined, and similar immunophenotypic characteristics were noted (data not shown).

Next, we examined the time course of the expression of CD19 in human BM CD34$^+$ cells in our culture system. CD19$^+$ cells were already detected after 1 week of culture (data not shown), and the number of CD19$^+$ cells increased throughout the course of the cell culture thereafter. After 4 to 9 weeks of culture, both the fluorescent intensity of CD19 on each cell and the percentage of CD19$^+$ cells out of the total number of cells continued to increase (Fig. 1E), but the total number of CD19$^+$ cells did not change significantly (data not shown). When expression of transcription factors related to early B-cell differentiation was analyzed by RT-PCR, expression profiles of these factors were well correlated with proliferation of CD19$^+$ cells as described (data not shown). Therefore, pro–B-cell development after 4 weeks of culture in the present system was analyzed in the following experiments.

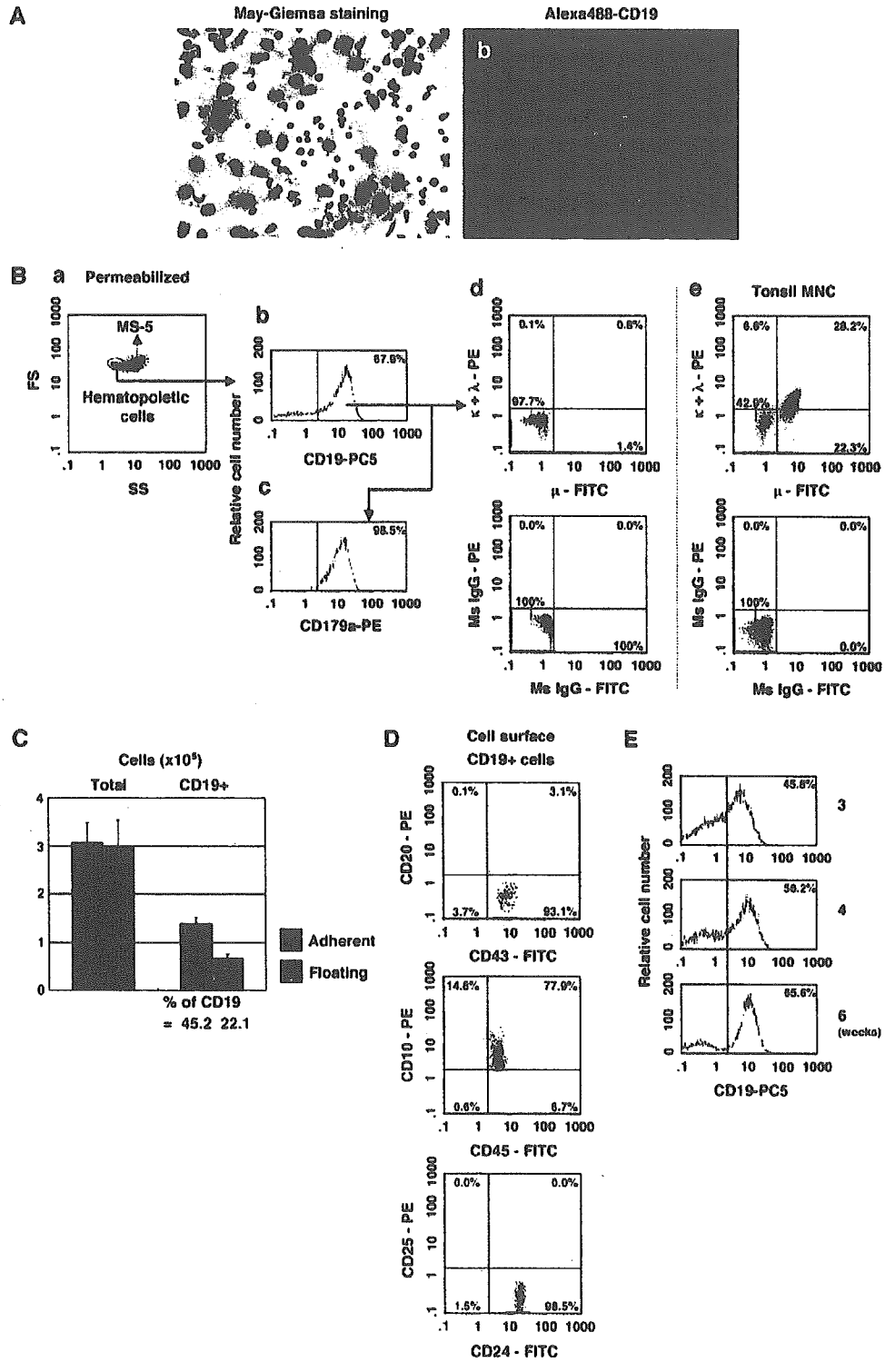
A
May-Giemsa staining
Alexa488-CD19
b
B a Permeabilized
MS-5
Hematopoietic cells
FS
SS
b
67.9%
CD19-PC5
Relative cell number
c
98.5%
CD179a-PE
d
0.1%
0.6%
97.7%
1.4%
κ + λ - PE
μ - FITC
0.0%
0.0%
100%
100%
Ms IgG - PE
Ms IgG - FITC
e
Tonsil MNC
6.6%
28.2%
42.9%
22.3%
κ + λ - PE
μ - FITC
0.0%
0.0%
100%
0.0%
Ms IgG - PE
Ms IgG - FITC
C
Cells (x10⁵)
Total
CD19+
Adherent
Floating
% of CD19
= 45.2 22.1
D
Cell surface
CD19+ cells
0.1%
3.1%
3.7%
93.1%
CD20 - PE
CD43 - FITC
14.6%
77.9%
0.6%
6.7%
CD10 - PE
CD45 - FITC
0.0%
0.0%
1.5%
98.5%
CD25 - PE
CD24 - FITC
E
45.6%
3
59.2%
4
85.6%
6
(weeks)
Relative cell number
CD19-PC5

Effect of IGF-I on in vitro human pro–B-cell development

Because expression of IGFRs in cultured $CD34^+$ BM cells was detected (Fig. 2A), we first tested the effect of adding exogenous recombinant human IGF-I to the coculture of $CD34^+$ BM cells and MS-5 cells to evaluate the contribution of IGF-I to human pro–B-cell development; no significant change in pro–B-cell development was observed (data not shown).

However, RT-PCR analysis revealed expression of IGF-I in MS-5 cells (Fig. 2B). Results of ELISA further demonstrated that mouse IGF-I was indeed secreted in the culture supernatant of MS-5 cells (Fig. 2C). As presented in Figure 2D, mouse IGF-I is active in human hematopoietic cells and can induce tyrosine-phosphorylation of human IGF-IR expressed on NALM-16 cells derived from human B-precursor acute lymphoblastic leukemia. When we tested similarly, MS-5 culture supernatant could stimulate IGF-IR on NALM-16 cells, whereas freshly prepared medium containing 10% FCS could not, indicating that mouse IGF-I secreted from MS-5 cells is sufficient to stimulate human hematopoietic cells. Therefore, the data suggest a possibility that MS-5 cells secrete excess amounts of IGF-I and thus exogenous addition of recombinant IGF-I revealed no effect on pro–B-cell development.

Indeed, when anti-mouse IGF-I Ab, which neutralizes the effect of IGF-I, was added to the culture, development of $CD19^+$ B cells was significantly reduced (Fig. 3A and B). As shown in Figure 3B, the initial addition of 5 μg/mL polyclonal goat anti-mouse IGF-I Ab was sufficient to induce a significant reduction in pro–B-cell development. When hamster anti-mouse IGF-I mAb was used, however, additional Abs were required to produce a remarkable reduction in subsequent pro–B-cell production (Fig. 3A). In both cases, anti-mouse IGF-I Abs not only reduced the total cell number of cultured $CD34^+$ BM cells, but also remarkably diminished the percentage of $CD19^+$ B cells out of the total number of cells in the culture. Therefore, reduction in $CD19^+$ B cells is not merely the result of an overall cell reduction. Moreover, anti-mouse IGF-I Ab-induced reduction in $CD19^+$ B-cell development was cancelled by the addition of recombinant human IGF-I (Fig. 3D). The data suggests that IGF-I significantly participates in pro–B-cell development. Evidence that anti-human IGF-IR Ab and IGF-IR kinase inhibitor, both of which can block the effect of IGF-I, reduce pro–B-cell development, further supports this notion (Fig. 3B and C).

Of note, RT-PCR analysis also showed a time-dependent expression of IGF-I in a total cell fraction, but not sorted $CD19^+$ cell fraction, of the cultured human BM $CD34^+$ cells during the culture period (Fig. 2A). Beside $CD19^+$ cell fraction, $CD33^+$ myelomonocytic cells were present in the culture (data not shown). Although $CD33^+$ cell population was decreasing with the culture time, they matured with time. Thus, time-dependent expression of IGF-I is most likely due to this cell fraction.

Effect of recombinant human IGFBPs on human pro–B-cell development

To assess the effect of IGFBPs on human pro–B-cell development, we challenged the present culture system with recombinant human IGFBPs. As shown in Figure 4A, of the six IGFBP members, only IGFBP-3 produced a subsequent reduction in the number of pro-B cells; the other IGFBPs did not affect human pro–B-cell development. As shown in Figure 4B, the inhibitory effect of IGFBP-3 on pro–B-cell differentiation was dose-dependent. Furthermore, IGFBP-3–mediated inhibition of $CD19^+$ cell development was cancelled by the addition of recombinant human IGF-I (Fig. 4C).

Because none of the IGFBPs other than IGFBP-3 affected pro–B-cell development from $CD34^+$ BM cells cocultured with MS-5, we tested a synergistic effect of two or more IGFBPs; no significant synergism was observed and other IGFBPs failed to enhance the effect of IGFBP3 (data not shown). Therefore, we next examined the effect of neutralization of the IGFBP function using specific Abs.

First we tested expression of IGFBPs in MS-5 cells. As shown in Figure 5A and B, RT-PCR experiments revealed that MS-5 transcribe mRNA of IGFBP-4, 5, and 6, but not 1, 2, and 3, while immunoblotting experiments using commercially available Abs detected only IGFBP-6 protein

Figure 1. Characterization of human bone marrow (BM) $CD34^+$ cells cocultured with murine stromal cells. (**A**) Human BM $CD34^+$ cells were cocultured for 4 weeks with murine stromal MS-5 cells on cover slips. At the end of the culture period, the cells were examined with either May-Grünwald-Giemsa staining (**a**) or CD19 immunostaining (green) with nuclear counter staining by 4′,6-diamidino-2-phenylindole (blue) (**b**). Original magnification ×400. (**B**) Human BM $CD34^+$ cells cocultured for 9 weeks with MS-5 cells were harvested. The expression of cell surface CD19, κ/λ light chains and cytoplasmic CD179a and μ heavy chain was simultaneously assessed by flow cytometry with cell-permeabilization technique as described in Materials and Methods. In cultured BM cells (**a**), $CD19^+$ cells were gated (**b**), and expression of CD179a (**c**), μ heavy chain, and κ/λ light chains (**d**) was examined. As a negative control, same sample specimen stained with isotype-matched control mouse IgG was also presented. As a positive control, mononuclear cells prepared from tonsil were similarly treated as in (**d**) and presented (**e**). FITC = fluorescein isothiocyanate; FS = forward light scatter; SS = side light scatter. (**C**) Human BM $CD34^+$ cells were cocultured with MS-5 cells for 4 weeks and the adherent cell fraction and floating cell fraction were collected separately. Total cell number and expression of CD19 were examined as above. (**D**) Human BM $CD34^+$ cells were cocultured with MS-5 cells as in (**B**), and multicolor immunofluorescence study was performed as above. $CD19^+$ cells were gated, and expression of surface B-cell differentiation markers, as indicated, was examined using flow cytometry. (**E**) Human BM $CD34^+$ cells were cocultured with MS-5 cells for 3, 4, and 6 weeks, and expression of CD19 was examined using flow cytometry.

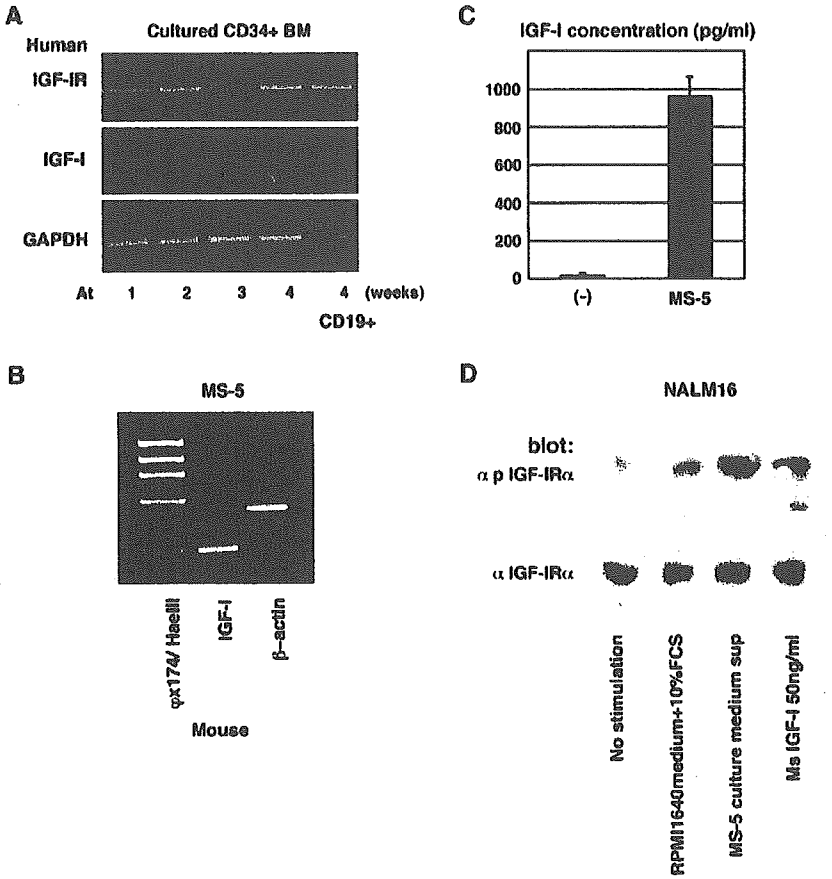

Figure 2. Expression of insulin-like growth factors (IGFs) and IGF receptors on cultured human bone marrow (BM) $CD34^+$ cells and murine stromal MS-5 cells. (A) Human BM $CD34^+$ cells were cocultured with MS-5 cells for 1, 2, 3, or 4 weeks, as shown in Figure 1. At the end of the culture periods, the floating fraction of the cultured human BM cells was collected and expression of human IGF-I receptor (IGF-IR) and IGF-I was examined using reverse transcriptase polymerase chain reaction (RT-PCR). As an internal control, expression of human glyceraldehyde phosphate dehydrogenase was also examined. $CD19^+$ cells were sorted from 4-week cultured human BM $CD34^+$ cells and similarly examined ($CD19^+$). (B) Expression of mouse IGF-I in MS-5 cells was examined using RT-PCR. As an internal control, expression of mouse β-actin was also examined. The $\phi\chi174$/*Hae*III molecular weight marker was presented in the left side. (C) MS-5 cells were cultured alone for 4 weeks and the culture supernatant was collected. Subsequent concentration of mouse IGF-I secreted by MS-5 cells in culture supernatant was determined by enzyme-linked immunosorbent assay. As a negative control, freshly prepared medium containing 10% fetal calf serum (FCS) was also examined, and no significant crossreaction was observed. (D) Biological effect of mouse IGF-I secreted by MS-5 cells on human hematopoietic cells was examined using NALM-16 cells that express IGF-IR. Cells at logarithmic growth were stimulated for 5 minutes with either freshly prepared culture medium containing 10% FCS, MS-5 culture supernatant, or recombinant mouse IGF-I (final concentration at 50 ng/mL) and examined by immunoblotting using antiphosphospecific human IGF-IR Ab that only recognize the activated form of IGF-IR. As a control, anti-entire IGF-IR Ab was also used.

expression. Coincident with the results of immunoblotting, anti-IGFBP-2, 3, and 5 Abs did not affect MS-5–induced pro–B-cell development from $CD34^+$ BM cells (Fig. 5C). Interestingly, however, when anti-mouse IGFBP-6 Ab was added to the culture system, pro–B-cell development was significantly reduced (Fig. 5C). In addition, as shown in Figure 5D, the anti-mouse IGFBP-6 Ab–induced inhibition of pro–B-cell development was completely canceled by the addition of human IGFBP-6. In light of this data, we concluded that the IGFBP-6 produced by the MS-5 cells is essential for pro–B-cell development from $CD34^+$ BM cells.

Discussion

In the present study, when BM $CD34^+$ cells were cultured in the presence of the murine stromal cell line MS-5, pro-B cells, but not pre-B cells, were efficiently induced. MS-5 is well known to be capable of supporting B-cell development [14–17]. However, several different groups have reported this cell line to have distinct effects on induction of B cells. Coincident with our observation, Berardi et al. [14] showed that when human HPSCs derived from umbilical CB were cultured in the presence of MS-5, $CD10^+$, $CD19^+$, and cytoplasmic μ^- pro-B cells were generated [14]. In contrast, Nishihara et al. [15] and Hirose et al. [16] reported the

induction of pre-B cells from CB CD34$^+$ cells after coculturing with MS-5 in the presence of exogenous granulocyte colony-stimulating factor (G-CSF) and stem cell factor (SCF) [14–16]. Moreover, Ohkawara et al. [17] reported that surface IgM$^+$ mature B cells could be produced from CB CD34$^+$ cells using the same culture condition. We tested the effect of the exogenous addition of G-CSF and SCF in our culture system, but failed to observe any signs of pre–B-cell differentiation (data not shown). Although a precise reason for such a difference is unavailable, it may be possible that different stocks of MS-5 exhibit distinct effects on B-cell differentiation. A comparison of the distinct effects of different MS-5 stocks on B-cell differentiation may provide useful and interesting information.

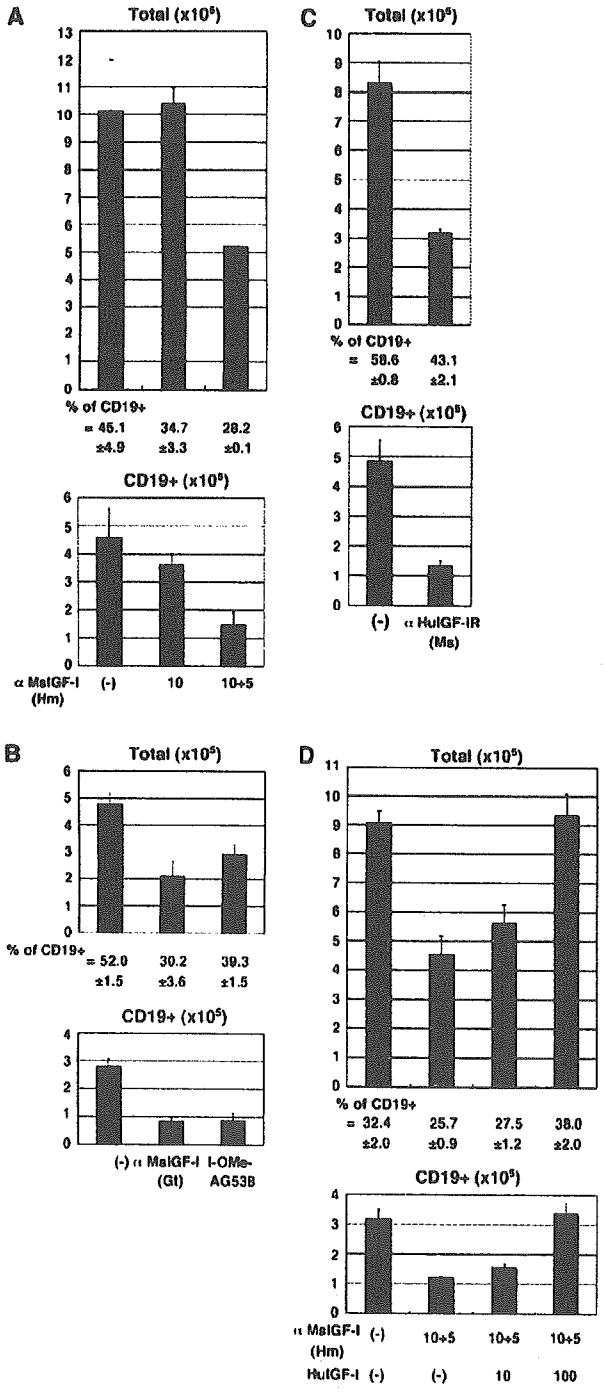

It was previously reported that earlier stages of B-cell development depend on contact with the stromal cells [15,17]. Consistently, culture supernatant of MS-5 cells failed to support pro–B-cell development from CD34$^+$ BM cells (data not shown), suggesting that cell-to-cell interaction between CD34$^+$ BM cells and MS-5 cells is essential for pro–B-cell development in our culture system. In contrast, however, we detected pro-B cells not only in adherent cell fraction, but also in floating cell fraction, while pro-B cells were more enriched in adherent cell fraction. Therefore, once have differentiated into pro-B cells, [Q8] contact with stromal cells may not always be necessary for further differentiation and/or proliferation and a portion of pro-B cells will dissociate from stromal cells and move to floating cell fraction.

As demonstrated in the present study, the MS-5 cells produced IGF-I, and elimination of IGF-1 function resulted in the failure of pro–B-cell development. Previous reports have revealed that IGF-1 is essential for differentiation of pro-B to pre-B cell [6,18] and expansion of B-cell population [7,8]. Therefore, our data extends previous observations and indicates that IGF-1 likely plays an important role in induction of pro-B cells from HPSCs.

As we presented in Figure 2A, IGF-1 is possibly secreted by a non–B-cell fraction of the cultured CD34$^+$ cells. IGF-1 may also be present in the supplemented FCS. Therefore, in addition to the IGF-1 secreted by MS-5 cells, IGF-1 produced by a non–B-cell fraction of the cultured CD34$^+$ cells as well as that provided by supplemented FCS can also affect to pro–B-cell development. However, as we presented in Figure 2D, the biological assay has indicated that the contribution of IGF-1 that may be present in the supplemented FCS can be exclude. Furthermore, because the [Q9] Abs used to neutralize IGF-1 activity in this study have higher specificity for mouse IGF-I than human IGF-I, it is

Figure 3. Effect of insulin growth factor-I (IGF-I) inhibition on human pro–B-cell development. Human bone marrow (BM) CD34$^+$ cells were cocultured with MS-5 for 4 weeks in the presence or absence of hamster anti-mouse IGF-I monoclonal antibody (mAb) [(A) α MsIGF-1 (Hm), either initial administration of 10 μg/mL alone (10) or a combination of an initial administration of 10 μg/mL and an additional administration of 5 μg/mL after 2 weeks of culture (10 + 5)], goat polyclonal anti-mouse IGF-I Ab [(B) α MsIGF-1 (Gt), 5 μg/ml)], IGF-IR kinase inhibitor I-OMe-AG538 [(B) 5 μM], mouse anti-human IGF-IR mAb [(C) α HuIGF-IR (Ms), 5 μg/mL], and a combination of α MsIGF-1 (Hm) and human IGF-I (HuIGF-1, 10, and 100 ng/mL) (D). Subsequent CD19$^+$ cell number was estimated using flow cytometry and is shown. Total cell number of cultured CD34$^+$ cells and the percentage of CD19$^+$ cells are also presented.

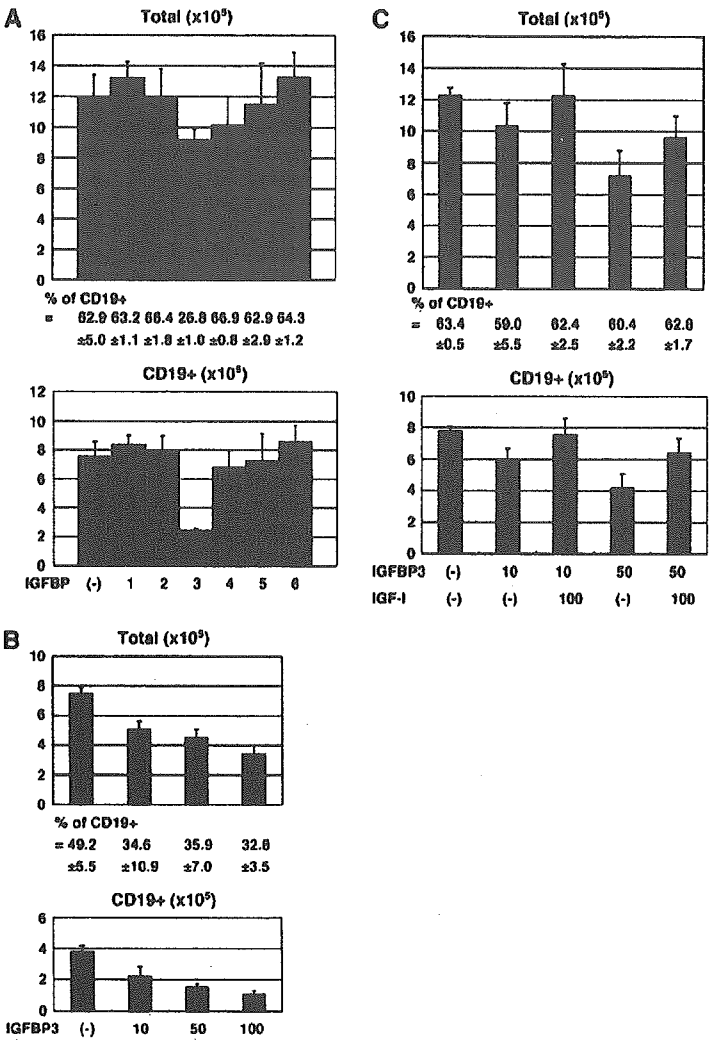

Figure 4. Effect of insulin-like growth factor (IGF)-binding proteins on human pro–B-cell development. (A) Human bone marrow (BM) $CD34^+$ cells were cocultured with MS-5 cells with or without 100 ng/mL each recombinant human IGF-binding proteins (IGFBP 1–6) for 4 weeks. The subsequent total cell number of cultured $CD34^+$ cells and the percentage and cell number of $CD19^+$ cells are shown. (B) Human BM $CD34^+$ cells were cocultured with MS-5 cells with or without different doses (ng/mL) of recombinant human IGFBP-3, as indicated, for 4 weeks and examined using the protocol described in (A). (C) Human BM $CD34^+$ cells were cocultured with MS-5 cells with or without indicated combinations of recombinant human IGFBP-3 (ng/mL) and human IGF-1 (ng/mL) and examined using the protocol described in (A).

most likely that the majority of IGF-1–mediated effects in our culture system are due to mouse IGF-1 secreted by MS-5 cells.

Because IGF-1 is thought to play an integrating role in hematopoiesis, it seems reasonable to consider that IGFBPs may also contribute to regulation of hematopoiesis. Evidence that IGFBPs are produced by stromal cells in the BM, yolk sac, and liver, where hematopoiesis occurs [19,20], strongly supports this notion. Indeed, a recent report by Liu et al. [21] suggested that IGFBP-3 may block differentiation of HPSCs and be capable of promoting proliferation of primitive $CD34^+CD38^-$ hematopoietic cells, contributing to expansion of the HPSC pool [21]. In this study, we further demonstrated that addition of exogenous IGFBP-3 inhibited the effect of IGF-1 on pro–B-cell induction from $CD34^+$ BM cells. Although MS-5 cells do not express IGFBP-3, it has been reported that BM stromal cells produce IGFBP-3 upon stimulation with several factors, such as vitamin D3 and transforming growth factor (TGF)-β1 [22,23]. Therefore, it is conceivable that IGFBP-3 could be secreted by BM stromal cells and involved in the regulation of early hematopoiesis, including B-cell development, depending on conditions in the hematopoietic microenvironment.

As demonstrated in the present article, while all six members of the IGFBP family possess the ability to bind

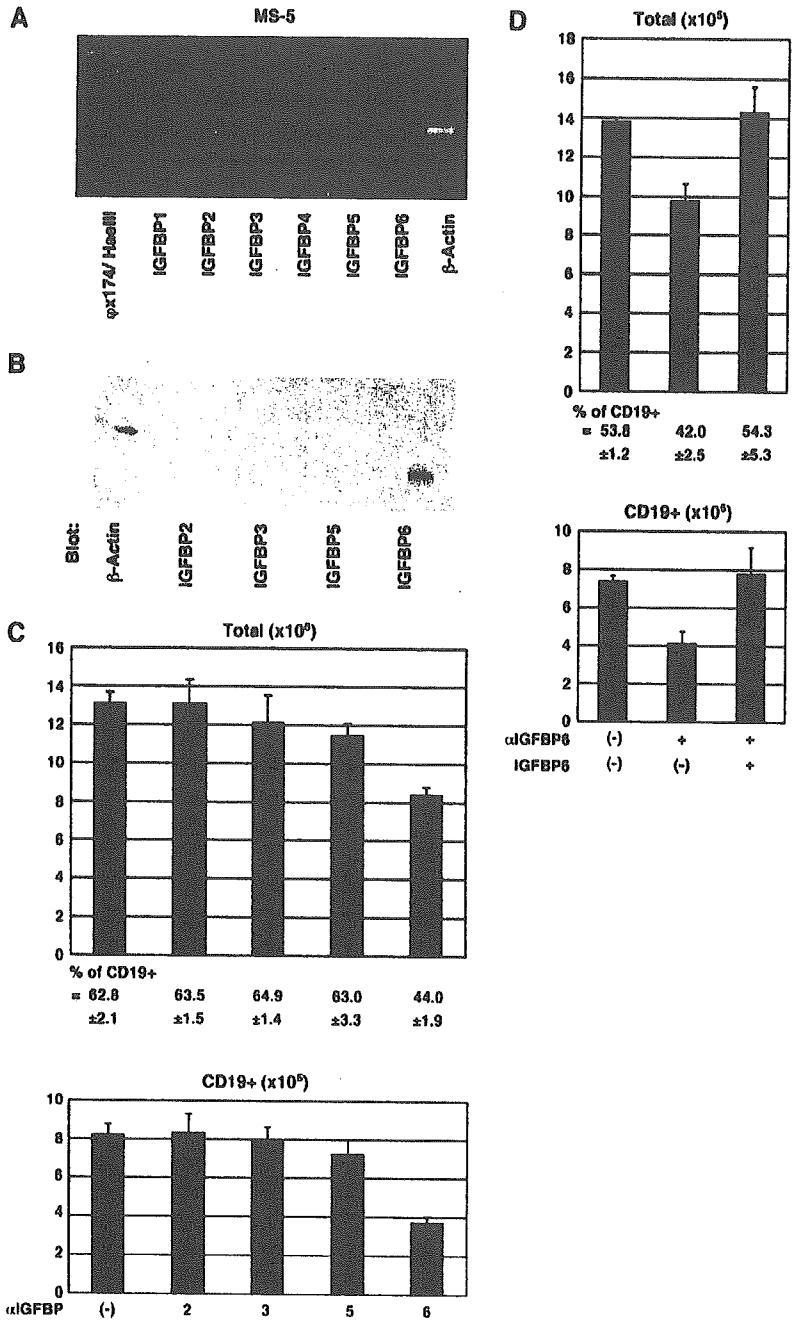

Figure 5. Effect of antibodies against insulin-like growth factor (IGF)-binding proteins on human pro–B-cell development. (A) Gene expression of mouse IGF-binding proteins (IGFBP) 1–6 on MS-5 cells was examined using reverse transcriptase polymerase chain reaction. As an internal control, expression of mouse β-actin was also examined. The $\phi\chi174/HaeIII$ molecular weight marker was presented in the left side. (B) Immunoblot analysis with goat anti-mouse IGFBP-2, 3 5, and IGFBP-6 antibodies (αIGFBP2-6, respectively) on MS-5 cell lysates was performed. (C) Human bone marrow (BM) $CD34^+$ cells were cocultured with MS-5 cells for 4 weeks with or without 10 μg/mL each goat antibodies against mouse IGF-binding proteins (αIGFBP), as indicated. Subsequent cell number of $CD19^+$ cells was examined using flow cytometry and is shown. Total cell number of cultured $CD34^+$ cells and percentage of $CD19^+$ cells are also presented. (D) Human BM $CD34^+$ cells were cocultured with MS-5 cells for 4 weeks with or without the indicated combination of αIGFBP6 (5 μg/mL) and recombinant human IGFBP-6 (100 ng/mL). Subsequent total cell number of cultured $CD34^+$ cells and percentage and cell number of $CD19^+$ cells was examined using the protocol described in (C).

with IGF, only IGFBP-3 inhibited the effect of IGF-1 on pro–B-cell development. Because all other IGFBPs failed to exert synergism with the IGFBP-3 in an inhibitory effect on pro–B-cell development in our experiment (data not shown), IGFBPs may compete with each other for binding with IGF-1, and IGFBP-3 should have the highest binding affinity. Furthermore, our data indicated that IGFBP-6 is required for pro–B-cell development, and neutralization of IGFBP-6 resulted in a marked reduction in the subsequent pro–B-cell number. Therefore, it is suggested that each IGFBP can have a distinct effect on the IGF action in regulation of hematopoiesis.

Interestingly, recent reports have indicated that IGFBPs have an intrinsic ability to affect cells directly [24–29]. For example, IGFBP-2 has been shown to be mitogenic in uterine endometrial and osteosarcoma cells in the absence of IGFs [30]. IGFBP-3 has been reported to induce a reduction in cell growth, DNA synthesis inhibition, and apoptosis in specific cells in an IGF-independent manner [31–34]. Furthermore, IGFBPs have been reported to have specific cell-surface receptors; IGFBP-2 and IGFBP-3 directly bind to target cells through $\alpha5\beta1$ integrin and TGF-β type-V receptors, respectively, thereby inducing intracellular signals [35,36]. Therefore, IGFBPs might not only inhibit the effects of IGF-1 during hematopoiesis, but also have intrinsic and direct bioactivities that directly affect hematopoietic cells independently of IGF-1 function.

In conclusion, IGF-1 and IGFBPs appear to play important roles in early B-lymphopoiesis. Although details of their molecular functions remain uncertain, IGFBPs can possibly affect hematopoietic cells in both IGF-dependent and IGF-independent manners. The present observations should contribute to a better understanding of the functional roles of IGF-1 and IGFBPs in regulation of B-lymphopoiesis.

Acknowledgments

We thank S. Yamauchi for her excellent secretarial work. We also thank Dr. A. Manabe, Dr. K. J. Mori, and Dr. Y. Matsuo for gifting murine BM stromal cell line, MS-5, and human leukemia cell line HPB-NULL. This work is supported in part by MEXT. KAKENHI 16017321, JSPS. KAKENHI 17591131, the Budget for Nuclear Research of the Ministry of Education, Culture, Sports, Science and Technology, based on the screening and counseling by the Atomic Energy Commission, grant from the Japan Health Sciences Foundation for Research on Health Sciences Focusing on Drug Innovation, and a Grant for Child Health and Development from the Ministry of Health, Labour and Welfare. T. Taguchi is an Awardee of Research Resident Fellowship from the Foundation for Promotion of Cancer Research (Japan) for the 3rd Term Comprehensive 10-Years-Strategy for Cancer Control.

References

1. Clark R. The somatogenic hormones and insulin-like growth factor-1: stimulators of lymphopoiesis and immune function. Endocr Rev. 1997; 18:157–179.
2. Baxter RC. Insulin-like growth factor (IGF)-binding proteins: interactions with IGFs and intrinsic bioactivities. Am J Physiol. 2000;278: E967–E976.
3. Rajaram S, Baylink DJ, Mohan S. Insulin-like growth factor-binding proteins in serum and other biological fluids: regulation and functions. Endocr Rev. 1997;18:801–831.
4. Firth SM, Baxter RC. Cellular actions of the insulin-like growth factor binding proteins. Endocr Rev. 2002;23:824–854.
5. Kurtz A, Matter R, Eckardt KU, Zapf J. Erythropoiesis, serum erythropoietin, and serum IGF-1 in rats during accelerated growth. Acta Endocrinol (Copenh). 1990;122:323–328.
6. Landreth KS, Narayanan R, Dorshkind K. Insulin-like growth factor-1 regulates pro-B cell differentiation. Blood. 1992;80:1207–1212.
7. Gibson LF, Piktel D, Landreth KS. Insulin-like growth factor-1 potentiates expansion of interleukin-7-dependent pro-B cells. Blood. 1993; 82:3005–3011.
8. Jardieu P, Clark R, Mortensen D, Dorshkind K. In vivo administration of insulin-like growth factor-1 stimulates primary B lymphopoiesis and enhances lymphocyte recovery after bone marrow transplantation. J Immunol. 1994;152:4320–4327.
9. Melchers F, Karasuyama H, Haasner D, et al. The surrogate light chain in B-cell development. Immunol Today. 1993;14:60–68.
10. Kiyokawa N, Kokai Y, Ishimoto K, Fujita H, Fujimoto J, Hata J. Characterization of the common acute lymphoblastic leukemia antigen (CD10) as an activation molecule on mature human B cells. Clin Exp Immunol. 1990;79:322–327.
11. Takenouchi H, Kiyokawa N, Taguchi T, et al. Shiga toxin binding to globotriaosyl ceramide induces intracellular signals that mediate cytoskeleton remodeling in human renal carcinoma-derived cells. J Cell Sci. 2004;117:3911–3922.
12. Saito M, Kiyokawa N, Taguchi T, et al. Granulocyte colony-stimulating factor directly affects human monocytes and modulates cytokine secretion. Exp Hematol. 2002;30:1115–1123.
13. Kiyokawa N, Lee EK, Karunagaran D, Lin S-Y, Hung M-C. Mitosis-specific negative regulation of epidermal growth factor receptor, triggered by a decrease in ligand binding and dimerization, can be overcome by overexpression of receptor. J Biol Chem. 1997;272: 18656–18665.
14. Berardi AC, Meffre E, Pflumio F, et al. Individual CD34+ CD38lowCD19-CD10- progenitor cells from human cord blood generate B lymphocytes and granulocytes. Blood. 1997;89:3554–3564.
15. Nishihara M, Wada Y, Ogami K, et al. A combination of stem cell factor and granulocyte colony-stimulating factor enhances the growth of human progenitor B cells supported by murine stromal cell line MS-5. Eur J Immunol. 1998;28:855–864.
16. Hirose Y, Kiyoi H, Itoh K, Kato K, Saito H, Naoe T. B-cell precursors differentiated from cord blood CD34+ cells are more immature than those derived from granulocyte colony-stimulating factor-mobilized peripheral blood CD34+ cells. Immunology. 2001;104:410–417.
17. Ohkawara JI, Ikebuchi K, Fujihara M, et al. Culture system for extensive production of CD19+IgM+ cells by human cord blood CD34+ progenitors. Leukemia. 1998;12:764–771.
18. Funk PE, Kincade PW, Witte PL. Native associations of early hematopoietic stem cells and stromal cells isolated in bone marrow cell aggregates. Blood. 1994;83:361–369.
19. Clawson TF, Lee WH, Yoder MC. Differential expression of insulin-like growth factor binding proteins in murine hematopoietic stromal cell lines. Mol Cell Endocrinol. 1996;120:59–66.
20. Abboud SL, Bethel CR, Aron DC. Secretion of insulinlike growth factor I and insulinlike growth factor-binding proteins by murine bone marrow stromal cells. J Clin Invest. 1991;88:470–475.
21. Liu LQ, Sposato M, Liu HY, et al. Functional cloning of IGFBP-3 from human microvascular endothelial cells reveals its novel role in promoting proliferation of primitive CD34+CD38- hematopoietic cells in vitro. Oncol Res. 2003;13:359–371.

22. Kveiborg M, Flyvbjerg A, Eriksen EF, Kassem M. 1,25-Dihydroxyvitamin D3 stimulates the production of insulin-like growth factor-binding proteins-2, -3 and -4 inhuman bone marrow stromal cells. Eur J Endocrinol. 2001;144:549–557.
23. Kveiborg M, Flyvbjerg A, Eriksen EF, Kassem M. Transforming growth factor-beta1 stimulates the production of insulin-like growth factor-I and insulin-like growth factor-binding protein-3 in human bone marrow stromal osteoblast progenitors. J Endocrinol. 2001; 169:549–561.
24. Valentinis B, Bhala A, DeAngelis T, Baserga R, Cohen P. The human insulin-like growth factor (IGF) binding protein-3 inhibits the growth of fibroblasts with a targeted disruption of the IGF-I receptor gene. Mol Endocrinol. 1995;9:361–367.
25. Oh Y, Muller HL, Lamson G, Rosenfeld RG. Insulin-like growth factor (IGF)-independent action of IGF-binding protein-3 in Hs578T human breast cancer cells. Cell surface binding and growth inhibition. J Biol Chem. 1993;268:14964–14971.
26. Oh Y, Muller HL, Pham H, Rosenfeld RG. Demonstration of receptors for insulin-like growth factor binding protein-3 on Hs578T human breast cancer cells. J Biol Chem. 1993;268:26045–26048.
27. Rajah R, Valentinis B, Cohen P. Insulin-like growth factor (IGF)-binding protein-3 induces apoptosis and mediates the effects of transforming growth factor-beta1 on programmed cell death through a p53- and IGF-independent mechanism. J Biol Chem. 1997;272: 12181–12188.
28. Conover CA, Bale LK, Durham SK, Powell DR. Insulin-like growth factor (IGF) binding protein-3 potentiation of IGF action is mediated through the phosphatidylinositol-3-kinase pathway and is associated with alteration in protein kinase B/AKT sensitivity. Endocrinology. 2000;141:3098–3103.
29. Rajah R, Lee KW, Cohen P. Insulin-like growth factor binding protein-3 mediates tumor necrosis factor-alpha-induced apoptosis: role of Bcl-2 phosphorylation. Cell Growth Differ. 2002;13:163–171.
30. Slootweg MC, Ohlsson C, Salles JP, de Vries CP, Netelenbos JC. Insulin-like growth factor binding proteins-2 and -3 stimulate growth hormone receptor binding and mitogenesis in rat osteosarcoma cells. Endocrinology. 1995;136:4210–4217.
31. Villaudy J, Delbe J, Blat C, Desauty G, Golde A, Harel L. An IGF binding protein is an inhibitor of FGF stimulation. J Cell Physiol. 1991;149:492–496.
32. Imbenotte J, Liu L, Desauty G, Harel L. Stimulation by TGF beta of chick embryo fibroblasts—inhibition by an IGFBP-3. Exp Cell Res. 1992;199:229–233.
33. Cohen P, Lamson G, Okajima T, Rosenfeld RG. Transfection of the human IGFBP-3 gene into Balb/c fibroblasts: a model for the cellular functions of IGFBPs. Growth Regul. 1993;3:23–26.
34. Bernard L, Babajko S, Binoux M, Ricort JM. The amino-terminal region of insulin-like growth factor binding protein-3, (1-95)IGFBP-3, induces apoptosis of MCF-7 breast carcinoma cells. Biochem Biophys Res Commun. 2002;293:55–60.
35. Schutt BS, Langkamp M, Ranke MB, Elmlinger MW. Intracellular signalling of insulin-like growth factor binding protein-2 [abstract]. Growth Horm IGF Res. 2000;0. A29.
36. Leal SM, Liu Q, Huang SS, Huang JS. The type V transforming growth factor beta receptor is the putative insulin-like growth factor-binding protein 3 receptor. J Biol Chem. 1997;272:20572–20576.

Available online at www.sciencedirect.com
SCIENCE DIRECT®
Biochemical and Biophysical Research Communications 332 (2005) 1004–1011
BBRC
www.elsevier.com/locate/ybbrc

Laminin binding protein, 34/67 laminin receptor, carries stage-specific embryonic antigen-4 epitope defined by monoclonal antibody Raft.2

Yohko U. Katagiri [a,b,*], Nobutaka Kiyokawa [a], Kyoko Nakamura [c], Hisami Takenouchi [a], Tomoko Taguchi [a], Hajime Okita [a], Akihiro Umezawa [d], Junichiro Fujimoto [a]

[a] *Department of Developmental Biology, National Research Institute for Child Health and Development, Setagaya-ku, Tokyo 157-8535, Japan*
[b] *Japan Science and Technology Corporation, CREST, Japan*
[c] *Supra-Biomolecular System Research Group, RIKEN Frontier System Research, Wako-shi, Saitama 351-0198, Japan*
[d] *Department of Reproductive Biology, National Research Institute for Child Health and Development, Setagaya-ku, Tokyo 157-8535, Japan*

Received 24 April 2005
Available online 23 May 2005

Abstract

We previously produced monoclonal antibodies against the detergent-insoluble microdomain, i.e., the raft microdomain, of the human renal cancer cell line ACHN. Raft.2, one of these monoclonal antibodies, recognizes sialosyl globopentaosylceramide, which has the stage-specific embryonic antigen (SSEA)-4 epitope. Although the mouse embryonal carcinoma (EC) cell line F9 does not express SSEA-4, some F9 cells stained with Raft.2. Western analysis and matrix-assisted laser desorption ionization-time of flight mass spectrometry identified the Raft.2 binding molecule as laminin binding protein (LBP), i.e., 34/67 laminin receptor. Weak acid treatment or digestion with *Clostridium perfringens* sialidase reduced Raft.2 binding to LBP on nitrocellulose sheets and [^{14}C]galactose was incorporated into LBP, indicating LBP to have a sialylated carbohydrate moiety. Subcellular localization analysis by sucrose density-gradient centrifugation and examination by confocal microscopy revealed LBP to be localized on the outer surface of the plasma membrane. An SSEA-4-positive human EC cell line, NCR-G3 cells, also expressed Raft.2-binding LBP.

Keywords: SSEA-4; SialylGb5; Embryonal carcinoma; Laminin binding protein; Laminin receptor; Raft.2; MALDI-TOF MS

EC derived from testicular teratocarcinomas are a subset of germ cell tumors that may contain many embryonic and extra-embryonic tissues, and they represent malignant replicas of normal embryonic cells at specific stages of development. Immunochemical markers, such as SSEA-1, -3, and -4, TRA-1-60, and TRA-1-81, have been utilized to characterize and define the developmental stages of EC lines. For example, early cleavage-stage mouse embryos [1] and the primitive and visceral yolk sac endodermal cells of post-implantation mouse embryos [2] express SSEA-3 and SSEA-4. These carbohydrate antigens are also found on human, but not on murine, EC cells [3]. By contrast, murine EC cells express SSEA-1, while human EC cells do not. Exposure to retinoic acid can prompt EC cells to develop to advanced stages, accompanied by changes in SSEA expressions. Many monoclonal antibodies defining SSEAs were generated in early studies of mammalian development. SSEA-1 is an antigenic epitope defined as a Lewis x (Le^x) carbohydrate structure and is found in both glycosphingolipids and glycoproteins [1,4]. SSEA-3 and -4 defined by MC631 and MC813-70, respectively,

* Corresponding author. Fax: +81 3 3487 9669.
E-mail address: kata@nch.go.jp (Y.U. Katagiri).

0006-291X/$ - see front matter © 2005 Elsevier Inc. All rights reserved.
doi:10.1016/j.bbrc.2005.05.052

are located in carbohydrate moieties of globoseries glycosphingolipids [5].

We previously established a monoclonal antibody (Mab) termed Raft.2 by subcutaneously injecting the raft microdomain of a human renal cancer cell line, ACHN, into Balb/c mice and showed that Raft.2 recognizes the carbohydrate structure of sialosyl globopentaosylceramide (sialylGb5), namely GL7, the epitope of SSEA-4 [6]. SSEAs are still among the best markers for characterizing embryonic stem (ES) cells or EC cells and Raft.2 is a potentially useful tool for this purpose.

Although mouse EC F9 cells are known to be SSEA-4 negative, some of these cells stained with Raft.2. In this study, we demonstrated that Raft.2 binds to LBP and that Raft.2-positive LBP is present not only in F9 cells, but also in human EC NCR-G3 cells. We also show LBP to be localized on surface membranes and discuss the significance of LBP carrying SSEA-4. This is the first report, to our knowledge, focusing the SSEA-4 carried by LBP.

Materials and methods

Cell culture and antibodies. The mouse EC cell line F9 and the human renal cancer cell line ACHN were purchased from the American Type Culture Collection. F9 cells were cultured in Dulbecco's modified Eagle's medium (DMEM) (Sigma Chem., St. Louis, MO) supplemented with 10% fetal bovine serum (Sigma). ACHN was cultured in Eagle's minimum essential medium (MEM) (Sigma) supplemented with 10% fetal bovine serum and the non-essential amino acid solution (Sigma). The human EC cell line, NCR-G3 [7], was cultured in a 1:1 mixture of DMEM and Ham's F12 medium (Gibco, Grand Island, NY) supplemented with 10% fetal bovine serum, insulin–transferrin–sodium selenite media (Sigma), and the non-essential amino acid solution. MC-631, Mab for SSEA-3 and MC-813-70, Mab for SSEA-4, to detect Gb5 and sialylGb5, respectively, were purchased from Chemicon International (Temecula, CA). 13C4, Mab for Shiga toxin 1-B subunit (Stx1B), and T-20, a rabbit anti-mouse GTP binding protein β subunit (Gβ) polyclonal antibody, were purchased from the American Type Culture Collection and Santa Cruz Biotechnology (Santa Cruz, CA), respectively.

Glycolipid analysis. The packed cell pellet (0.5 ml) was extracted with 2 ml chloroform/methanol (C/M) (2:1, v/v) and then with 2 ml of chloroform/isopropanol/water (7:11:2, v/v). Total extracts were combined and evaporated to dryness and then treated with 0.2 N KOH in methanol at 37 °C for 2 h to saponify the phospholipids. After neutralization, methyl esters of fatty acids were removed by mixing with hexane. The extracts were then concentrated to 1/10 volume and dialyzed against water. The retentate was freeze-dried and dissolved in C/M (2:1).

Thin layer chromatography (TLC) immunostaining was performed according to a previously described method [8]. Briefly, C/M extracts were separated on plates precoated with Silica gel 60 (HPTLC aluminium sheets, Merck, Darmstadt Germany) using a solvent system consisting of C/M/water containing 0.1% $CaCl_2$ (5:4:1, v/v/v). After drying, the plates were dipped in 0.1% polyisobutylmethacrylate (Aldrich Chem., Milwaukee, WI, USA) in cyclohexane for 1 min and blocked with 1% bovine serum albumin (BSA) in phosphate-buffered saline (PBS). The plates were probed with Shiga toxin 1-B subunit (Stx1B) (1 μg/ml in 1% BSA) [9], then Mab 13C4 culture supernatant to detect globotriaosylceramide (Gb3), and with Mab Raft.2 culture supernatant to detect sialylGb5. After three washes with PBS for 5 min each, horseradish peroxidase-conjugated rabbit anti-mouse immunoglobulins (DAKO, A/S, Denmark) at a 1:2000 dilution ratio were used as the second antibody. The antibodies that bound to the plates were visualized with enhanced chemiluminescence reagent SuperSignal (Pierce, Rockford, IL, USA) and detected by LAS-1000 (Fuji Film, Tokyo, Japan).

Flowcytometry. Cells were harvested and incubated with a 1st antibody for 1 h on ice, followed by treatment with fluorescein isothiocyanate-conjugated goat anti-mouse immunoglobulins (Jackson Laboratory, West Grove, PA) at a 1:50 dilution ratio and analyzed by flowcytometry (EPICS-XL, Beckman–Coulter).

Western analysis. Cells were homogenized in hypotonic buffer (25 mM NaCl, 0.5 mM $CaCl_2$, 18 mM Tris–HCl buffer, pH 8.0) and cell debris was removed by centrifugation at 200*g* for 5 min at 4 °C. Precipitates were homogenized in the same manner two more times. The combined supernatants were centrifuged at 40K rpm for 30 min at 4 °C in a Beckman 80Ti rotor to obtain crude membrane fractions. The membrane proteins released with 1% Triton X-100 in 25 mM Tris–HCl buffer, pH 7.5, containing 0.15 M NaCl and the cocktail of protease inhibitors, were subjected to 1-dimensional (1-D) or 2-D Western analysis as previously described [10]. In order to remove the sialic acids from the glycoproteins, after 1-D Western blotting, the membrane strips were treated with 25 mM H_2SO_4 at 80 °C for 1 h.

Matrix-assisted laser desorption ionization-time of flight mass spectrometry (MALDI-TOF MS) analysis. The membrane proteins were separated by 2-D polyacrylamide gel electrophoresis (PAGE) and stained with Coomassie brilliant blue (CBB) R-250 (Bio-Rad Lab., Richmond, CA). The CBB-stained protein that corresponded to the position of the Raft.2-reacting spot was excised and digested with trypsin, and the trypsinized peptides were analyzed with an oMALDI-Qq-TOF MS/MS QSTAR Pulser *i* (Applied Biosystems). The mass spectra search was conducted using an NCBI non-reductant database with the MASCOT search algorithm.

Metabolic labeling of F9 cells with [^{14}C]galactose. Subconfluent cells (approx. 1.4×10^6 cells) were cultured in 4 ml of the incubation medium containing 10 μCi D-[1-^{14}C]galactose (57 mCi/mmol, 200 μCi/ml, Amersham Biosciences UK) for 24 h in a 60 mm culture plate. [^{14}C]Galactose-labeled membrane protein was prepared as above and mixed with 50 μg of non-labeled F9 membrane proteins. The F9 membrane protein mixture thus obtained was separated by 2-D PAGE and stained with CBB. Autoradiograms were obtained with BAS 2000.

Sialidase treatment. Proteins on 2-D nitrocellulose sheets were stained with Ponceau 3R Stain Solution (Wako Pure Chem., Osaka, Japan) and the rectangle containing the proteins of interest was excised. The blots were incubated in 50 mM sodium acetate buffer, pH 4.5, containing 0.1% BSA, with or without 100 mU of neuraminidase from *Clostridium perfringens* (Roche Diagnosis GmbH, Mannheim, Germany) at 37 °C overnight.

Subcellular fractionation. Crude membrane fractions obtained as described above were thoroughly suspended in the hypotonic buffer containing 30% sucrose and overlaid on a discontinuous sucrose density gradient of 40%/45%/50%/60% in a 12-ml ultracentrifugation tube, and the suspension was then overlaid with a 20% sucrose layer. The gradient was centrifuged at 25K rpm for 1 h in a Beckman SW40Ti rotor, and after recovery and dilution with PBS, each of the interface layers was sedimented at 40K rpm for 0.5 h in a Beckman 80Ti rotor. Proteins were released from each precipitate with 1% Triton X-100 lysis buffer and subjected to 2-D PAGE.

Staining for fluorescence microscopic observation. EC cells were harvested from cell culture plates and incubated with Raft.2. They were then stained with Alexa Fluor 488-conjugated goat anti-mouse IgM, μ-chain (Molecular probes, Eugene, OR) for 1 h and mounted in Perma Fluor Aqueous Mounting Medium (Thermo Shandon, Pittsburgh, PA) on a slide glass. The slides were observed with an Olympus LSM-GB200 confocal microscope.

Results

The sialylGb5 expressions on murine and human EC cells were examined by TLC immunostaining and flowcytometry with two Mabs against SSEA-4, Raft.2, and MC-813-70. ACHN cells, which express globoseries glycolipids, such as Gb3 and sialylGb5, were also examined and compared, as a control. All of these cell lines synthesized Gb3 (Fig. 1A, left panel). SialylGb5 was synthesized by ACHN and NCR-G3, but not F9, cells (Fig. 1A, right panel). ACHN and NCR-G3 cells were confirmed to express both sialylGb5 and Gb5 on their surface by flowcytometry (Fig. 1B, upper and lower row). Flowcytometric analysis further confirmed SSEA-4 expression on small populations (8.42%+) of F9 cells using Raft.2 and the faint expression using MC-813-70 (Fig. 1B, middle row). The staining profile of MC-631 was similar to that of Raft.2 (6.7%+). Taking these observations together, although F9 cells do not synthesize sialylGb5, they clearly express the SSEA-4 epitope on their surfaces.

We performed Western analysis to ascertain whether the SSEA-4-carried molecules are glycoproteins. Cytoplasmic proteins and 1% Triton membrane lysates of F9 cells were subjected to 1-D and 2-D Western analysis. Mab Raft.2 definitely bound to a membrane protein with an apparent molecular weight (mw) of 44K (Fig. 2A), but did not bind to cytoplasmic proteins (data not shown). Since Raft.2 cannot bind to Gb5, sialic acid residue is prerequisite for Raft.2 binding to the SSEA-4 epitope. Weak acid treatment of the blot markedly diminished Raft.2 binding to the 44K protein, while only minimally decreasing T-20 binding to its antigen, Gβ. These findings indicate that the carbohydrate chain of the protein is sialylated. 2-D Western analysis yielded

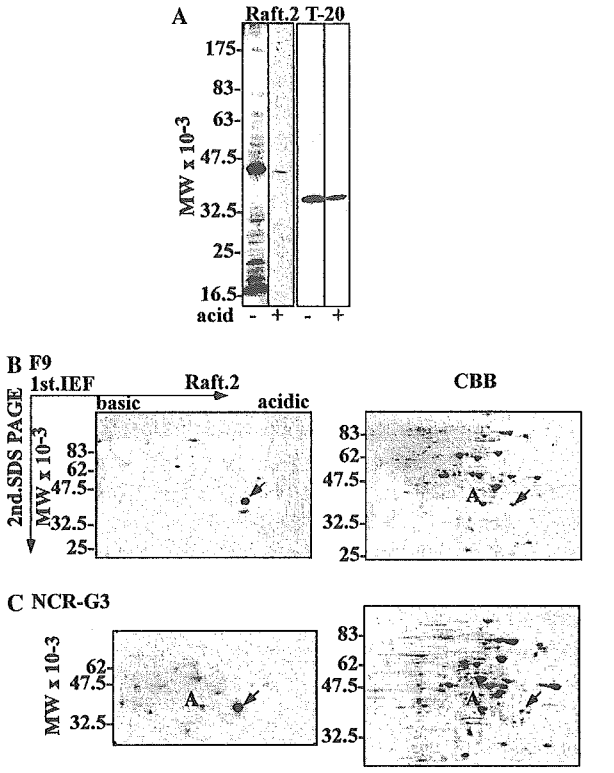

Fig. 2. Western analysis of the Raft.2 binding protein. (A) Membrane proteins of F9 cells were separated to four lanes by 1-D SDS–PAGE and transferred to a nitrocellulose sheet. Two of the strips were treated with weak acid (+), the other two were not (−). Two (− and +) were probed with Raft.2 (left), the other two with T-20 (right). (B) The membrane proteins separated by 2-D PAGE were transferred to a nitrocellulose sheet and probed with Raft.2 (left panel) or the membrane proteins in a 2-D gel were stained with CBB (right panel). The arrow points to the spot bound by Raft.2 and "A" indicates actin. (C) Membrane proteins of NCR-G3 cells were analyzed as in (B).

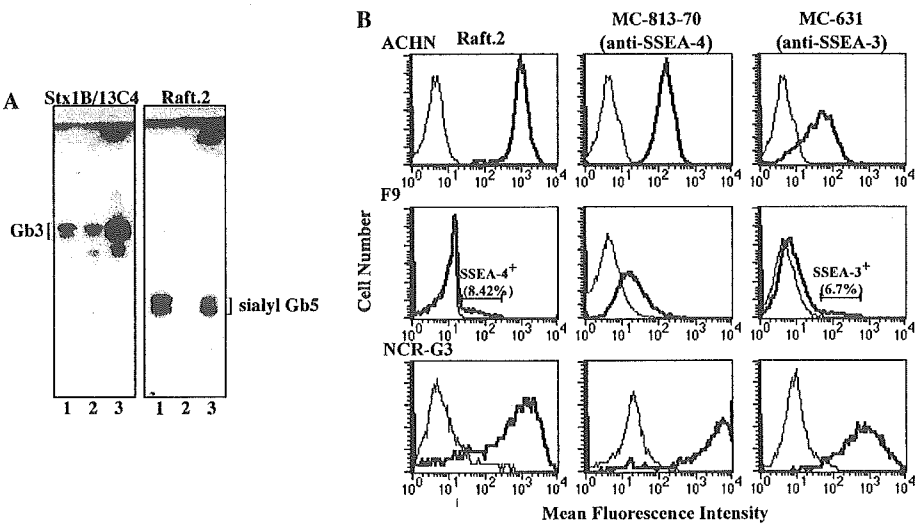

Fig. 1. Expression of SSEA-4 by the murine and human EC cell lines, F9 cells, and NCR-G3. (A) Total lipids from ACHN cells (lane 1), F9 cells (lane 2), and NCR-G3 cells (lane 3) were separated by TLC and immunostained with Stx1B/13C4 (left) and Raft.2 (right). (B) Cells were stained with Raft.2 (left row), MC-813-70 (middle row), or MC-631 (right row) and with a FITC-conjugate secondary antibody and analyzed by flowcytometry.